Materials Science & Engineering A 734 (2018) 224–228

Contents lists available at ScienceDirect

Materials Science & Engineering A

journal homepage: www.elsevier.com/locate/msea

Short communication

Dislocation-stacking fault interactions in a nanostructured Al alloy processed by severe plastic deformation

Zhigang Yan[a], Yaojun Lin[a,b,*]

[a] State Key Laboratory of Metastable Materials Science and Technology, Yanshan University, Qinhuangdao, Hebei 066004, China
[b] School of Materials Science and Engineering, Wuhan University of Technology, Wuhan, Hubei 430070, China

ARTICLE INFO

Keywords:
Stacking fault
Dislocation
Nanostructured materials
Aluminum alloy
Severe plastic deformation
High-pressure torsion

ABSTRACT

Experimental observations on dislocation-stacking fault (SF) interactions in nanostructured (NS) Al and Al alloys have received very limited attention albeit some available theoretical studies using molecular dynamic simulations in the published scientific literature; consequently, the effect of the SFs on strength and ductility remains poorly understood. In an effort to address this question, the present study reports a type of configurations comprising one or several full dislocation(s) and a SF in a NS Al alloy processed by high-pressure torsion. The configurations were identified and studied using high resolution transmission electron microscopy. The calculations reveal that the two partial dislocations enclosing the SF generate high magnitudes of components of stress in the position of the full dislocation(s), indicative of strong full dislocation-SF interactions. This finding suggests the potential of the SFs to enhance both strength and ductility of NS Al and Al alloys by impeding dislocation slip and entrapping dislocations.

1. Introduction

Over the past two decades, the microstructural features in the nanostructured (NS) and ultra-fine grained face-centered cubic (FCC) metals and alloys with medium to high stacking fault energy, especially twins and stacking faults (SFs) that can be rarely observed in their coarse-grained (CG) counterparts, have been widely studied [1–6]. These studies have been primarily motivated not only by the presence of the two microstructural features as the indications of unique deformation mechanisms [1–6] but also by their effects on mechanical properties including strength and ductility [2,7–9]. It has been well documented that the presence of twins can simultaneously improve strength and ductility of NS metals and alloys, which originates from the dislocation interactions with and accumulations at, twin boundaries [5,6,10]. In order to provide insight into the underlying mechanisms, the dislocation-twin interactions have been extensively studies experimentally [5,10–12] and theoretically [6,13]. However, inspection of the published scientific literature shows that, to date, the studies on dislocation-SF interactions have received very limited attention. In a related study [14,15], Yamakov et al. investigated the interaction between a dislocation and an extrinsic SF in NS Al using molecular dynamics (MD) simulations, revealing that the dislocation can pass through the extrinsic SF. In another related study by Wei et al., the MD simulations of the interactions between a screw dislocation and SFs in NS FCC metals show that the screw dislocation can either annihilate the intrinsic and extrinsic SFs or pass through them, depending on the stacking fault energy and stress level. In view of the above discussion, there is lack of experimental studies on dislocation-SF interactions. In an effort to solve this problem, a NS FCC Al alloy processed by high-pressure torsion (HPT) was investigated using transmission electron microscopy (TEM) and high resolution TEM (HRTEM) in the present study. A type of configurations comprising one or several full dislocation(s) and a SF were observed. By calculating the stress field(s) in the position of the full dislocation(s) that are generated by the two partial dislocations in the SF, the dislocation-SF interactions were analyzed and discussed.

2. Materials and methods

A widely used commercial 7075 Al alloy with the composition of Al-2.4Zn-2.9Mg-0.67Cu-0.14Cr (at%) was implemented in the present study. The alloy was first solution treated at 480 °C for 5 h, and then quenched to room temperature in water. A disk with a thickness of 0.8 mm and a diameter of 10 mm was subjected to HPT for 10 revolutions under an applied pressure of 6 GPa with a rotation rate of 0.2 revolution per minute. Microstructure in the as-HPT alloy was characterized via TEM and HRTEM (model: Fei-ETEM) operated at 200 kV. The TEM/HRTEM specimens were prepared by mechanical grinding to

* Corresponding author at: School of Materials Science and Engineering, Wuhan University of Technology, Wuhan, Hubei 430070, China.
E-mail address: yjlin@whut.edu.cn (Y. Lin).

https://doi.org/10.1016/j.msea.2018.07.102
Received 6 May 2018; Received in revised form 26 July 2018; Accepted 27 July 2018
Available online 29 July 2018
0921-5093/

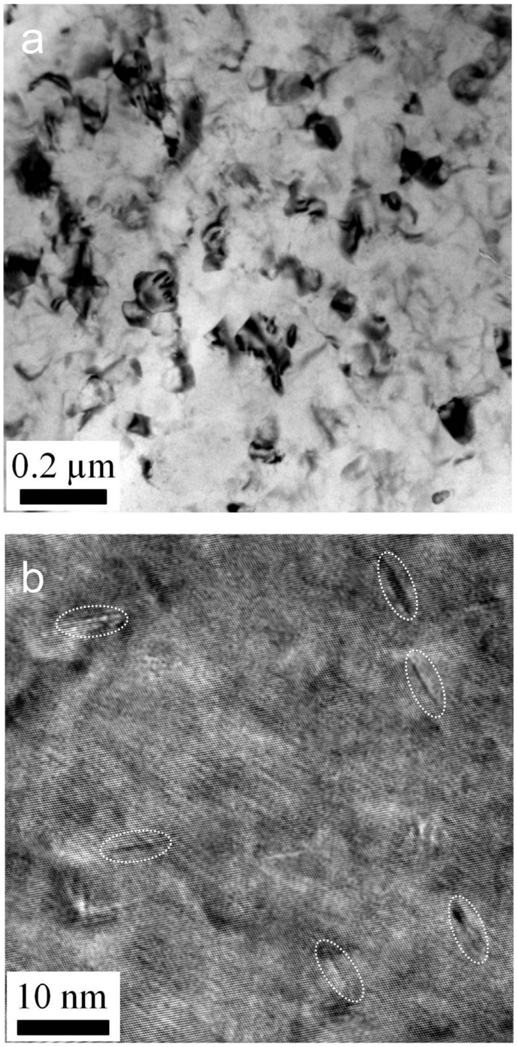

Fig. 1. (a) The typical TEM BF micrograph of the HPT Al alloy, showing microstructure with grain sizes ranging from 20 to 180 nm, and (b) the HRTEM micrograph of a nano-sized grain, showing the presence of SFs marked using ellipses.

20–30 µm in thickness followed by twin-jet polishing to electron transparency using a solution of 5 vol% perchloric acid and 95 vol% ethanol at −20 °C.

3. Results

Fig. 1 demonstrates the typical planar-view TEM bright field (BF) micrograph of the NS Al alloy processed by HPT. Fig. 1a shows grain sizes ranging from ~ 20 to ~ 180 nm, with the average grain size being ~ 80 nm. The HRTEM micrograph of a nano-sized grain is displayed in Fig. 1b, showing a high density of intragranular SFs as marked using the white ellipses. Based on analysis of a series of HRTEM micrographs, the widths of SFs fall in the range from 1.2 to 6 nm with an average width of 2.7 nm, and the density of SFs is estimated to be ~ 2.4×10^{15} m^{-2}.

Careful inspection of Fig. 1b reveals the presence of full dislocations very close to some of the SFs. In a HRTEM micrograph obtained on the [110] axis as shown in Fig. 2a, a full dislocation F_2 marked using "T" can be observed, which is positioned very closely to a 2.9 nm wide SF enclosed by two partial dislocations P_{21} and P_{22} marked with "T". The distances between dislocations F_2 and P_{21}, and between dislocations F_2 and P_{22} are 0.51 nm and 3.25 nm, respectively. In order to discern the atomic images more clearly, the inverse fast Fourier transformation (IFFT) micrograph of Fig. 2a is also provided in Fig. 2b. By drawing

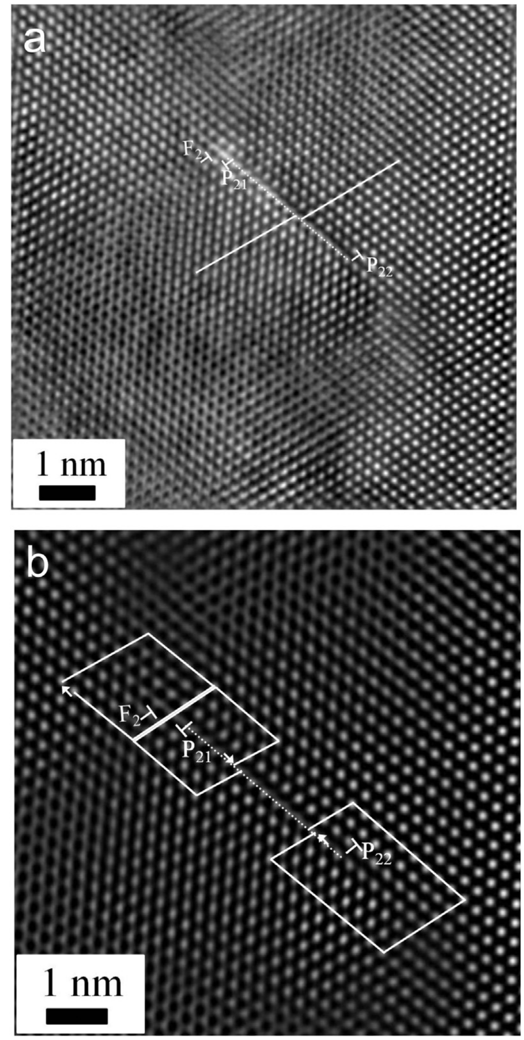

Fig. 2. The configuration comprising a full dislocation F_2 and a 2.9 nm wide SF enclosed by two partial dislocations P_{21} and P_{22}: (a) HRTEM micrograph with the SF and dislocations F_2, P_{21} and P_{22} marked using white "T", and (b) the IFFT micrograph of (a) with three Burgers circuits surrounding dislocations F_2, P_{21} and P_{22}.

Burger circuits surrounding the three dislocations in Fig. 2b, the projection vectors of their Burgers vectors on plane (110) can be measured as $\frac{1}{4}[1\bar{1}\bar{2}]\,a$, $\frac{1}{12}[\bar{1}12]\,a$ and $\frac{1}{12}[1\bar{1}\bar{2}]\,a$, where $a = 0.405$ nm is the lattice constant of Al, corresponding to dislocations F_2, P_{21} and P_{22}. Then, their Burgers vectors can be determined to be $\frac{1}{2}[10\bar{1}]\,a$, $\frac{1}{6}[121]\,a$ and $\frac{1}{6}[21\bar{1}]\,a$ by matching these measured projection vectors with the calculated ones of the Burgers vectors of all of the possible full and partial dislocations present in FCC Al that are shown in the well-established Thompson tetrahedron [16]. Inspection of the published scientific literature reveals that a dislocation can be clearly observed using HRTEM only if its dislocation line aligns very closely to the direction of the electron beam [17–19]. Hence, it is considered appropriate to assume the directions of the dislocation lines are along [110] for the three aforementioned dislocations. The relevant parameters in the configuration comprising the full dislocation and the SF are summarized in Table 1.

Fig. 3 shows another configuration that consists of two full dislocations F_{31} and F_{32} and a SF enclosed by two partial dislocations P_{31} and P_{32}, where these dislocations are marked using white "T", and the two full dislocations are positioned in the same side of the SF. In addition, a configuration containing three full dislocations F_{41}, F_{42} and F_{43} and a SF connecting two partial dislocations P_{31} and P_{32} are observed in Fig. 4, where all dislocations are marked using white "T". Full